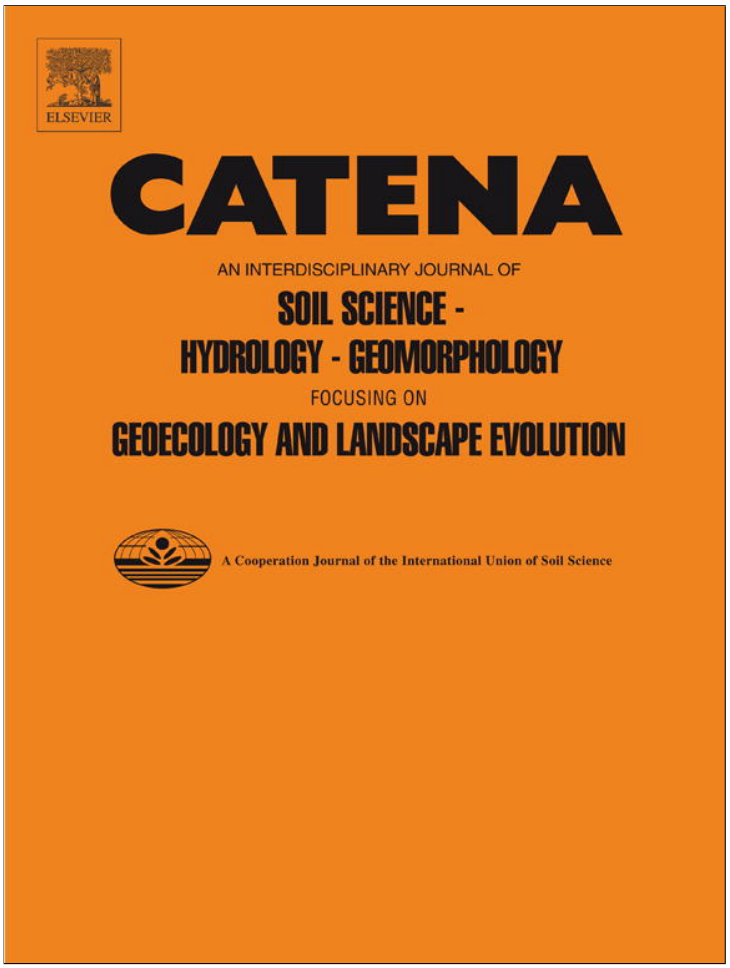

(This is a sample cover image for this issue. The actual cover is not yet available at this time.)

Catena 97 (2012) 50–62

Contents lists available at SciVerse ScienceDirect

Catena

journal homepage: www.elsevier.com/locate/catena

Soil nutrient dynamics during podzol development under lowland temperate rain forest in New Zealand

Benjamin L. Turner [a,*], Leo M. Condron [b], Andrew Wells [b], Kelly M. Andersen [a]

[a] Smithsonian Tropical Research Institute, Apartado 0843-03092, Balboa, Ancón, Panama
[b] Agriculture and Life Sciences, PO Box 84, Lincoln University, Lincoln 7647, Canterbury, New Zealand

ARTICLE INFO

Article history:
Received 3 June 2011
Received in revised form 2 May 2012
Accepted 16 May 2012
Available online xxxx

Keywords:
Chronosequence
Phosphorus
Nitrogen
Spodosol
Pedogenesis
Coastal dune

ABSTRACT

The Haast chronosequence on the west coast of the South Island of New Zealand consists of a series of coastal dune ridges formed by periodic earthquake disturbance over the last 6500 years. It approximates an ideal chronosequence, because soils are under the same climate and vegetation, have similar topography, and are developed in the same parent material. We assessed soil development and the changes in nutrients at eleven sites along the sequence to determine rates of nutrient transformations and the potential for limitation of biological activity by nitrogen and phosphorus availability. Soils develop rapidly to podzols (Spodosols) under the super-humid climate, involving acidification and depletion of base cations in the first few hundred years, development of a bleached eluvial horizon under a thick organic horizon within 2000 years, and formation of a continuous cemented iron pan within 4000 years. Soil phosphorus concentrations decline markedly in the first few hundred years in both the organic and upper mineral soil horizons, with rapid depletion of primary mineral phosphate and the accumulation of organic phosphorus to ~80% of the total phosphorus in the upper mineral soil. These changes lead to an increasing degree of phosphorus limitation along the sequence, as indicated by an increase in C:P and N:P ratios and a decline in available phosphate. The rates of soil development and phosphorus depletion are more rapid than at the nearby Franz Josef post-glacial chronosequence, where glacial moraine derived from graywacke contains a relatively high phosphorus concentration and weathers into fine-textured soils. The Haast chronosequence therefore provides an important additional example of soil development linked to long-term depletion of soil phosphorus under a perudic moisture regime.

Published by Elsevier B.V.

1. Introduction

Soil chronosequences provide a means of assessing the development of soils over time periods ranging from decades to millions of years (Stevens and Walker, 1970). An ideal chronosequence includes sites that differ only in the time since the onset of soil formation: all other soil forming factors should remain constant, including parent material, topography, climate, and vegetation. Well-studied examples of sequences that approximate this ideal include the Hawaiian Island chronosequence (Crews et al., 1995), the Franz Josef post-glacial chronosequence in New Zealand (Walker and Syers, 1976), the Lake Michigan dunes in the USA (Lichter, 1998), and the Cooloola sand dune chronosequence in eastern Australia (Thompson, 1981).

One of the key changes in soil properties during pedogenesis is the long-term decline in the availability of soil phosphorus (Wardle et al., 2004). This occurs through the gradual loss of total phosphorus via leaching and erosion (Hedin et al., 2003) and chemical transformations in the forms of phosphorus remaining in the soil (Walker and Syers, 1976). Specifically, inorganic phosphorus in primary minerals is depleted rapidly following the onset of pedogenesis, with an increasing predominance of phosphorus bound in secondary minerals and organic compounds (Crews et al., 1995; Parfitt et al., 2005; Turner et al., 2007). In contrast, nitrogen concentrations tend to be lowest in young soils and to increase during ecosystem development through the action of nitrogen fixing organisms (Menge and Hedin, 2009). These changes have important ecological implications, because the progressive increase in phosphorus limitation as soils age eventually leads to a decline in forest biomass on old, stable land surfaces (Wardle et al., 2004). These changes in soil nutrients and plant biomass appear be a widespread phenomenon, because the same pattern occurs in ecosystems that have developed on a range of geological substrates and under a range of climates (Peltzer et al., 2010). Yet despite the significance of soil chronosequences in aiding our understanding of long-term pedogenic processes and associated impacts on plant and microbial communities (Walker et al., 2010) there are only a limited number of sequences globally where retrogression occurs (Peltzer et al., 2010). Information on additional sequences is therefore required to strengthen our understanding of long-term ecosystem development.

Here we report the results of a detailed survey of soils along the Haast chronosequence, a progradational dune sequence formed by

* Corresponding author.
E-mail address: TurnerBL@si.edu (B.L. Turner).

0341-8162/$ – see front matter. Published by Elsevier B.V.
doi:10.1016/j.catena.2012.05.007

periodic disturbance events linked to earthquakes on the Alpine Fault that runs through the South Island of New Zealand (Wells and Goff, 2006, 2007). In many ways the Haast sequence approximates an ideal chronosequence: the dunes have similar morphology (although there is some variation in dune size), are formed from the same parent material, support undisturbed forest, and the dates of dune formation are reasonably well-constrained, particularly for the young dunes. Basal area measurements in the forest communities along the dune system indicate that it represents a retrogressive chronosequence (Turner et al., unpublished data). Our specific aims were to assess soil development along the Haast chronosequence and quantify associated changes in soil phosphorus and other nutrients that might be linked to limitation of biological activity. We were particularly interested in whether the rate of phosphorus depletion would correspond to that observed at the nearby and well-studied Franz Josef post-glacial chronosequence (Parfitt et al., 2005; Turner et al., 2007; Walker and Syers, 1976), a very different sequence in terms of parent material, soil properties and sequence age, but under similar rainfall and vegetation.

2. The Haast chronosequence

The Haast dune system is a foredune progradation sequence located a few km northeast of the town of Haast, on the west coast of the South Island of New Zealand (approximate center of the sequence 43°43′20″ S, 169°4′30″ E) (Fig. 1). Dune building episodes are thought to result from earthquakes along the Alpine Fault and/or prolonged periods of high rainfall, causing widespread land disturbance including landslides, rock falls, floodplain aggradation, and tree falls (Wells and Goff, 2007). After each event, a pulse of sediment is transported rapidly to the ocean via the Haast River, which carries one of the highest sediment loads of any river in the world (Griffiths, 1979). Sediment is then deposited as a linear dune either side of the mouth of the river. The youngest dune is thus located closest to the ocean, with dunes becoming progressively older inland. The Haast dune system extends ~10 km alongshore and 5 km inland, with dunes 20–100 m long rising up to 20 m above

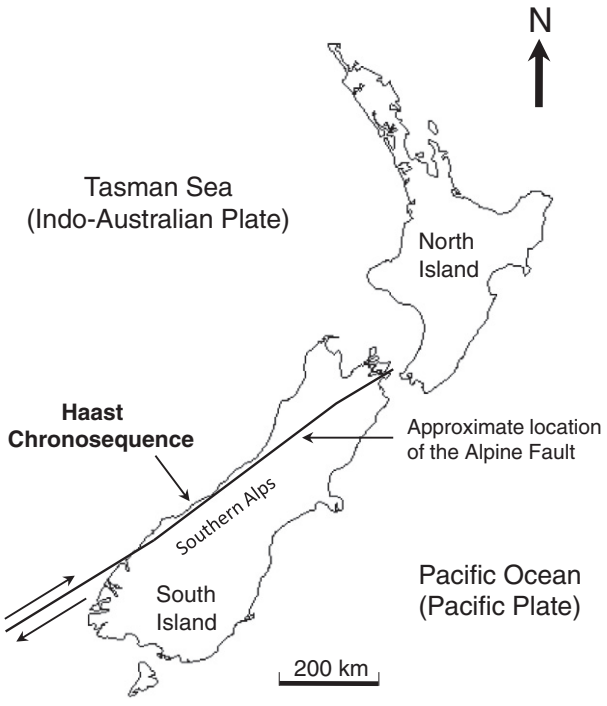

Fig. 1. The location of the Haast chronosequence, South Island, New Zealand. The map shows the approximate location of the Alpine Fault, which separates the Indo-Australian Plate from the Pacific Plate, with the Southern Alps located to the east of the fault. Periodic movement along the Alpine Fault leads to sediment pulses from the Southern Alps into the Tasman Sea and the formation of the dune features at Haast.

adjacent dune slacks. There are a total of seventeen dune ridges that occur as generally continuous features across the length of the system, although some are more prominent than others (Fig. 2).

2.1. Ages of dune formation

Dune building has occurred following all known Alpine Fault earthquakes since A.D. 1220 and is a regional phenomenon, with dunes of similar age occurring at multiple sites along the coastline (Wells and Goff, 2007). Dunes appear to have been forming in the region since sea level stabilized during the mid-Holocene, ca. 7000 years ago (Wells and Goff, 2006).

The earliest dunes have been dated precisely using tree rings and historical records. Wells and Goff (2007) reported dates for five dune sequences in the region, including the Haast sequence, with the oldest tree on each dune providing a minimum age for dune stabilization. At all sites, dune formation occurred within a short period of time following disturbance (10–50 years), interspersed with longer periods of inactivity. Actual stabilization dates pre-date the oldest trees by ca. 5–30 years, corresponding to the time required for colonization and growth to coring height (Wells and Goff, 2007).

Formation dates for the dunes studied here are summarized in Table 1. The most recent dune is dated precisely at A.D. 1826 from historical records. The A.D. 1717 and A.D. 1460 earthquakes appear to have caused the greatest impacts in the region over the past 600 years. The timing and causes of dune formation prior to A.D. 1460 are not as well documented, although the A.D. 1220 event is reasonably well constrained by tree-ring analysis and is most probably related to an Alpine Fault earthquake (Wells and Goff, 2007). It is also reasonable to assume that sedimentation episodes related to large earthquakes have played the dominant role in dune formation throughout the older parts of the dune sequence. The oldest dune is dated at ca. 6500 years before present by ^{14}C analysis of an organic sample located at the base of the peat column in the dune slack in front of the dune (personal communication of an unpublished date by Sean Fitzsimons, University of Otago, New Zealand). This age is broadly consistent with the expected timing of the onset of dune formation based on sea level maxima following the end of the last ice age, and suggests that the sequence began forming no earlier than about 7000 years before present (Wells and Goff, 2007).

Dunes between A.D. 1220 and the oldest dune (6500 years B.P.) have so far eluded accurate dating. In particular, luminescence dating of parent material (sand from the C horizon of soil profile pits) has proved inconclusive (A. Wells and J. Goff, unpublished data). For the purposes of this study we estimated the ages of Dunes 8–15 by dividing the number of years between Dune 6 and Dune 17 (i.e., 5713 years) by the total number of dunes after Dune 6 (i.e., 11 dunes), giving a mean age of 519 years between dunes (Table 1). This assumes a regular periodicity of dune formation, although luminescence dating and dune morphology both suggest a discontinuity after Dune 13; the oldest dunes are wider and separated by pronounced swales, which perhaps indicates that they were formed over longer periods of time and/or by multiple earthquake events.

2.2. Parent material

Lithology in the region near the main divide of the Southern Alps that contributes sediment load to the Haast River is predominantly well-foliated schist masses, including semi-schistose graywacke and argillite; this relatively weak rock is prone to slumps and failures following earthquake disturbance (Tonkin and Basher, 1990). The parent material is assumed to be similar across the dune sequence, although it is possible that differences in earthquake magnitude could affect the source material. A further possible source of variation is that the general northward movement of material by longshore drift may lead to sorting along the individual dunes and/or a difference between dunes formed

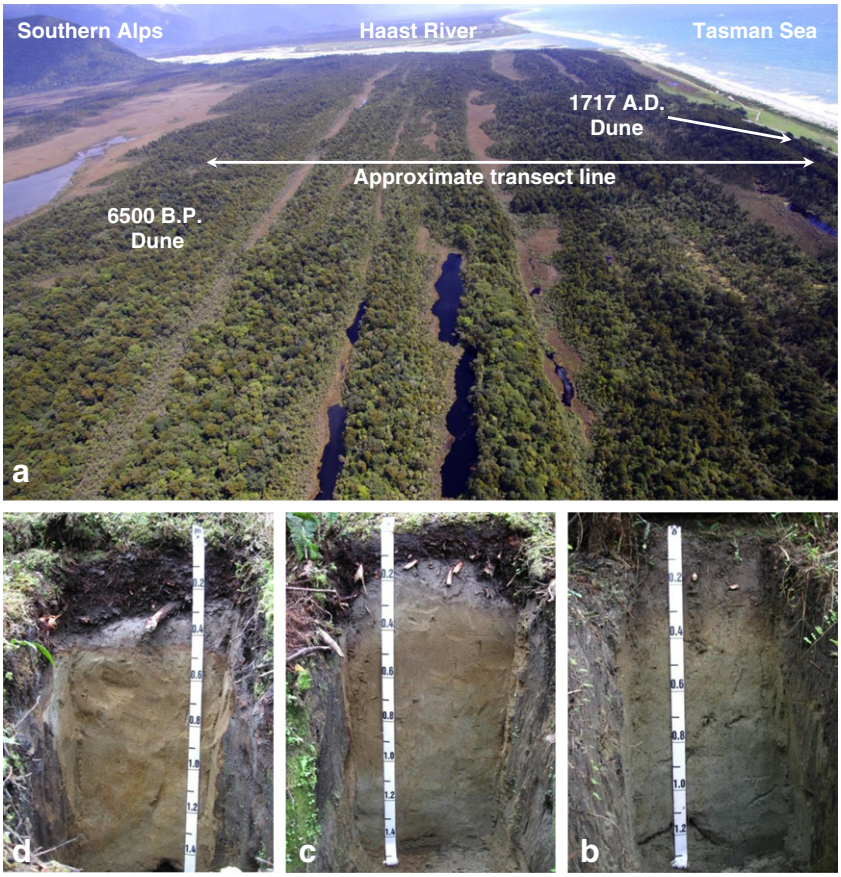

Fig. 2. (a) Aerial view of the Haast Chronosequence looking south towards the Haast River in the distance, with the youngest dunes on the right close to the ocean (indicated by Dune 2 formed following the 1717 A.D. earthquake) and the oldest dunes furthest inland (indicated by the 6500 B.P. dune). The approximate transect line across the sequence is between the two marked dunes. (b) A weakly developed soil (Typic Udipsamment) on a young dune (Dune 4; 517 years B.P). (c) A moderately-developed soil (Spodic Udipsamments) on an intermediate-aged dune (Dune 8; 1826 years B.P.), showing a clear bleached eluvial horizon under a thick organic horizon. (d) A well-developed Spodosol (Typic Placorthod) on an old dune (Dune 12; 3903 years B.P.), showing a bleached eluvial horizon, a spodic B horizon, and a continuous cemented placic horizon (iron pan). Photo credits: a, A. Wells; b–d, B.L. Turner.

Table 1
Dates for the dune stages analyzed in this study.

Dune stage	Disturbance type	Disturbance date	Dune age (years B.P.)[a]	Dating method
1	Fiordland earthquake[b]	A.D. 1826	181	Tree rings
2	Alpine Fault earthquake	A.D. 1717	290	Tree rings
3	Alpine Fault earthquake	A.D. 1615 ± 5.	392	Tree rings
4[c]	Alpine Fault earthquake	A.D. 1490 ± 10	517	Tree rings
6[d]	Alpine Fault earthquake	A.D. 1220 ± 15	787	Tree rings
8	Unknown	?	1826	Estimated
11	Unknown	?	3384	Estimated
12	Unknown	?	3903	Estimated
13	Unknown	?	4422	Estimated
15	Unknown	?	5461	Estimated
17	Unknown	B.C. 4500 ± 500	6500	^{14}C date

[a] Dates from year of first year of sampling (2007); ages for dune stages 1–6 from Wells and Goff (2007), stage 17 from a radiocarbon date (personal communication, Sean Fitzsimons, University of Otago, New Zealand), and stages 8–15 estimated by assuming an equal number of years between each dune stage for all dunes between stages 6 and 17.

[b] A subduction-zone earthquake (Wells et al., 2001).

[c] Earthquake dated at 1460, although Wells and Goff (2007) suggest two disturbance events in the region prior to 1450 and 1525. The earlier dune (Dune 5) may have been initiated as early as A.D. 1430, but was not included in the current study. Dune 4 has a minimum age from tree rings of A.D. 1506, suggesting a slightly earlier date of formation, so we estimate the dune formation date as A.D. 1490.

[d] On the north side of the river the dune for this stage is small and contained no remaining dateable first-generation trees. However, the dune occurs on a parallel system on the south side of the river that supports many dateable trees. For this study, soil was sampled from this dune on the south side of the river.

to the north and south of the river mouth. However, the particle size distribution of the parent sand is similar across the sequence (see below) and the mineralogy of the unweathered sand appears relatively uniform in differently-aged dunes, being 40–50% quartz, with the remainder feldspar, mica and chlorite (Palmer et al., 1986).

2.3. Climate

Based on the 36 year period between 1941 and 1976 (New Zealand Meteorological Service, 1983), mean annual rainfall at Haast Beach, close to the chronosequence, is 3455 mm. Rainfall is associated mainly with depression fronts and is spread relatively evenly throughout the year, with ≥1 mm rain falling on 178 days per year and no month having <200 mm. Mean annual temperature is 11.3 °C, with mean monthly values between 7.4 °C in July and 14.9 °C in February. Air frosts are rare (seven days per year), but there are ~55 days of ground frost per year. Relative humidity averages 83%.

Climate at the site has varied considerably since the onset of dune formation. Evidence from a variety of sources indicates a strong dry period in the South Island of New Zealand around 3000 to 4000 years B.P. (e.g., McGlone and Wilmshurst, 1999; Williams et al., 2004), which also influenced the Haast area (Li et al., 2008). There is also evidence for a substantial temperature decrease around 3500 years B.P., based on records of glacial movement (Gellatly et al., 1988), sea surface temperatures (e.g., Porter, 2000), and pollen records (Li et al., 2008). Evidence from glacial fluctuations indicates several cold periods during

the formation of the sequence, including: 5000, 4500–4200, 3700, 3500–3000, 2700–2200, 1800–1700, 1500, 1100, 900, 700–600 and 400–100 years B.P. (Gellatly et al., 1988).

2.4. Vegetation

Forests in the region are mixed conifer–broadleaf temperate rain forest, which have persisted in the lowlands since 7700 B.P., and probably since 11,400 B.P. (Li et al., 2008). The conifers consist of members of the family Podocarpaceae, which occur widely throughout New Zealand forests (Coomes and Bellingham, 2011). Prominent species include *Dacrydium cupressinum* (rimu), *Prumnopitys ferruginea* (miro), *Podocarpus hallii* (montane totara), and *Phyllocladus alpinus* (celery pine). Woody angiosperms in the area include *Weinmannia racemosa* (kamahi), *Coprosma* spp., *Metrosideros umbellata* (southern rata), and *Nothofagus menziesii* (silver beech), as well as the tree ferns *Dicksonia squarrosa* (wheki) and *Cyathea smithii* (pateke). The youngest dune has been largely cleared of forest and converted to pasture, but some low stature forest remains on the seaward dune crest. Detailed analysis of vegetation changes along the sequence will be reported elsewhere.

2.5. Topography

The dunes are of similar form throughout the sequence, being linear and generally continuous features. There is some variation in dune height; the majority of the dunes are 3–4 m above the surrounding dune slacks, but Dunes 6 and 17 are larger (~15 m), perhaps due to particularly disruptive earthquake events. Dune height is of potential significance in terms of depth to the water table.

3. Methods

3.1. Selection of dunes

We chose eleven clearly defined and continuous dune ridges for detailed study (Table 1). Some of the other dunes ridges were difficult to discern from the adjoining swales in places. The youngest dune (Dune 1, 181 years B.P.) is located to the west of the coast road adjacent to the modern beach and supports relatively short-stature vegetation. Dunes 2–4 were sampled along a short transect running inland from the road perpendicular to the coast. A fifth dune along this transect (Dune 5) dated to A.D. 1410 was not sampled because it is of relatively low stature at this site. Dune 6 (787 years B.P.) is also not well-represented north of the Haast River, and supports no dateable trees. We therefore studied this dune on the southwest side of the Haast River, where it occurs as a large dune similar in size to the oldest dune of the sequence (Dune 17, ~6500 years B.P.). Dunes 8–17 were sampled along a second transect that was approximately a continuation of the transect line for Dunes 2–4, although accessed from a trail slightly to the south of the first transect line.

3.2. Soil sampling and preparation

In February 2007 we sampled surface soils from three replicate 5 × 10 m plots located on ten of the eleven dunes (i.e., excluding Dune 15). Plots were located from the dune crest to the upper back-slope, as this represents the area of dune most likely to be stabilized initially. Ten replicate samples were taken in each plot with a 2.5 cm diameter soil probe and were separated into the organic horizon and the upper mineral soil (0–20 cm). This yielded three composite samples of organic soil and three of mineral soil for each dune. Mineral soil samples represented the A horizon on young dunes and E horizons on older dunes (see Supplementary Material). Field-moist samples were extracted for nitrogen and phosphate analysis (see below). The remaining samples were air-dried at 30 °C for 10 days. Subsamples were ground finely in a ball mill for total element analysis.

A soil profile pit was excavated to ~1.5 m on the back-slope of each of 11 dunes. Profiles were described and sampled by genetic horizons. Samples were taken from profile pits in 2007 during initial work at the site, and then subsequently in 2009 (both times in February). Soils were classified based on US Soil Taxonomy (Soil Survey Staff, 1999) in discussion with scientists at the Natural Resource Conservation Service (NRCS) in Lincoln, Nebraska, USA.

3.3. Determination of extractable nutrients

Exchangeable inorganic phosphate was determined by extraction with anion-exchange membranes. Extracted phosphate was recovered from membranes in 0.25 M H_2SO_4 and detected by automated molybdate colorimetry with in-line neutralization (Turner and Romero, 2009). The procedure extracts mainly inorganic phosphate, although some acid-labile organic and condensed inorganic phosphates may be included (Cheesman et al., 2010).

Extractable inorganic nitrogen (ammonium and nitrate) was determined on two occasions. In 2007, field-moist soils were extracted in 0.5 M K_2SO_4 after approximately 10 days storage, with detection of ammonium and nitrate by automated colorimetry on a Lachat Quickchem 8500 (Hach Ltd, Loveland, CO). Due to emerging concerns about the effects of storage on extractable nitrogen (Turner and Romero, 2009) we re-sampled soils in March 2008 from six sites (Dunes 1, 3, 4, 8, 13, 17) to 5 cm depth after removing leaf litter and extracted nitrogen in 2 M KCl in the field. Samples were filtered within 6 h of sampling, and ammonium and nitrate determined by a similar procedure to that described above.

Exchangeable cations were determined in each genetic horizon of the soil profiles by a single-step extraction in 0.1 M $BaCl_2$, with detection of Al, Ca, Fe, K. Mg, Mn, and Na by inductively-coupled plasma optical-emission spectrometry (ICP–OES) (Hendershot et al., 2008) using an Optima 7300DV spectrometer (Perkin Elmer Inc., Shelton, CT). Effective cation exchange capacity was calculated as the sum of extracted cations, with base saturation calculated as the proportion (%) of the effective cation exchange capacity accounted for by exchangeable bases (Ca, K, Mg, and Na).

3.4. Determination of other soil chemical and physical properties

Total phosphorus was determined by ignition (550 °C, 1 h) and extraction in 1 M H_2SO_4 (1:50 soil to solution ratio, 16 h), with orthophosphate detection in neutralized extracts at 880 nm by automated molybdate colorimetry using a Lachat Quickchem 8500 (Hach Ltd, Loveland, CO). This procedure gave quantitative recovery of total phosphorus from certified reference soil (Loam Soil D; High Purity Standards, Charleston, SC). In mineral soils, inorganic phosphorus was extracted from unignited samples in 1 M H_2SO_4, with phosphate detection as described above. The inorganic phosphorus was assumed to approximate primary mineral phosphate (i.e., apatite). We did not determine acid-extractable phosphate on organic horizon samples because these were not expected to contain apatite. The difference between total phosphorus and inorganic phosphate was assigned to organic phosphorus, although these values are likely to be overestimates given that secondary mineral phosphate can be solubilized by high temperature ignition (Williams and Walker, 1967).

Particle size analysis was determined by the pipette method following oxidation of organic matter by H_2O_2 and dispersion in sodium hexametaphosphate (Gee and Or, 2002). Soil pH was determined in a 1:2 soil to solution ratio in both deionized water and 10 mM $CaCl_2$ using a glass electrode. Moisture content was determined by drying for 24 h at 105 °C. Total carbon and nitrogen were determined by combustion and gas chromatography using a Thermo Flash NC1112 Soil Analyzer (CE Elantech, Lakewood, NJ). Oxalate-extractable aluminum, iron, manganese, and phosphorus were determined by extraction in a

solution containing ammonium oxalate and oxalic acid (Loeppert and Inskeep, 1996) with detection by ICP–OES.

3.5. Calculation of profile weights of carbon, nitrogen, and phosphorus

Total profile weights of C, N, and P were calculated to 1 m depth of the mineral soil for each profile pit from element concentrations and bulk density measured in each genetic horizon with a 10 cm diameter stainless steel cylinder. For organic horizons, element weights were calculated from element concentrations in composite samples from the three replicate plots on each dune, with depth of the organic layer measured at five points and bulk density determined by a constant volume cylinder.

4. Results

4.1. Soil development along the Haast chronosequence

Examples of the three main stages of soil development along the Haast chronosequence are shown in Fig. 2, with key diagnostic features (eluvial horizon, placic horizon, etc.) reported in Table 2. Detailed soil descriptions and full chemical and physical analyses by genetic horizon are provided in a supplementary file available online.

Young dunes (<800 years B.P.) were classified as Typic Udipsamments (Entisols) (Fig. 2a). Profiles on these dunes exhibited very dark grayish brown (10YR 3/2) A horizons 20–30 cm thick with weak blocky structure. There was some weak subsurface development, with light olive brown (e.g., 2.5Y 4/3 or 5/3) structureless B horizons 20–40 cm thick. The coarse sandy texture of these horizons precludes them from classification as cambic horizons. The C horizons were structureless (granular) olive gray (2.5Y or 5Y 4/3) sand.

Intermediate-aged dunes (1826–3384 years B.P.) were classified as Spodic Udipsamments (Entisols), based on the development of weak spodic B horizons (Fig. 2b). They were characterized by a pronounced thickening of the surface organic horizon and development of an albic (E, eluvial) horizon in the upper mineral soil. The formation of an albic horizon, characteristic of the early stages of podzolization, therefore occurred sometime between 787 and 1826 years after dune formation.

Older dunes (3903–6500 years B.P.) were classified as Typic Placorthods (Spodosols) based on the presence of an albic horizon, a spodic B horizon, and a placic horizon (cemented iron pan) (1c). The iron pan therefore formed after 3384–3903 years of pedogenesis, although this is speculative given that the dating of the older dunes is imprecise. The albic horizon occurred below a thick organic horizon and on the oldest three dunes the lower part of the albic horizon directly above the iron pan was enriched in organic matter and was therefore classified as a Bh horizon. The iron pan was 3–5 mm thick on Dune 12, but increased to ~10 mm thick on the older dunes.

There was some evidence of post-depositional disturbance on Dune 11 (3384 years B.P.) in the form of a buried albic horizon at 36 cm depth below the mineral soil surface, with more recent A and B horizons above. This presumably indicates the deposition of younger material at the surface following the development of the original albic horizon.

4.2. Soil chemical and physical properties along the chronosequence

Soils developed rapidly during the early stages of pedogenesis (Fig. 3). In upper mineral soils (0–20 cm), pH measured in water was already as low as 4.7 on the youngest dune (values for the beach sand were close to neutral) and decreased further to 4.2 by the next dune (290 years B.P.). Values then declined slowly to the lowest value of 3.6 on the oldest dune. Organic horizon pH values were more variable but followed a similar trend, with values measured in water being higher on young dunes <1000 years old (4.1–5.6) and lower on older dunes >1000 years old (3.7–4.1) (see Supplementary Material).

There was a general trend of increasing silt and clay concentrations in upper mineral horizons with soil development (Fig. 3), as indicated by topsoil texture measured in soil profile pits, varying from sand on young dunes to loamy sand on older dunes (Table 2). In the surface mineral soil, which corresponded to A horizons in young dunes and E or Bh horizons in older dunes, the sand content declined from 99% in the youngest dune to 78% in the oldest dune, the silt content was <10% on young dunes (<1000 years old) but 11–17% on older dunes, and the clay content was as low as 1% on the youngest dune but reached 5–8% on older dunes (>1000 years) (Fig. 3). The C horizons contained ≥99% sand-sized material (53–2000 μm) throughout the sequence (see Supplementary Material); the majority of this was coarse sand (200–2000 μm) (Palmer et al., 1986). This indicates that weathering was primarily responsible for increasing concentrations of clay in surface soils along the sequence, rather than variation in parent material.

Although exchangeable base cation concentrations were low throughout the sequence, there was a rapid depletion of exchangeable bases in the early stages of pedogenesis. Effective cation exchange capacity in surface mineral soil ranged between 2.6 and 8.3 $cmol_c\ kg^{-1}$ across the sequence, accounted for mainly by exchangeable aluminum (Table 2; Supplementary Table 1). Concentrations of exchangeable bases were slightly greater on young dunes compared to old dunes, although almost all calcium, potassium, and magnesium concentrations were <1 $cmol_c\ kg^{-1}$ (see Supplemental Material). In B horizons the exchange capacity was almost all accounted for by aluminum, with extremely low concentrations

Table 2
Description of soils from profile pits on each of eleven dune stages along the Haast dune sequence, New Zealand. Full profile descriptions and associated analytical results are reported in Supplementary Material.

Dune stage	Dune age (years B.P.)	Soil taxonomy	Eluvial (albic) horizon	Dune height	Iron pan (placic horizon)	Topsoil texture	Effective cation exchange capacity[a]	Total exchangeable bases[b]
			—cm—	—m—			—$cmol_c\ kg^{-1}$—	—%—
1	181	Typic Udipsamment	No	3	No	Sand	–	2.3
2	290	Typic Udipsamment	No	2	No	Sand	0.6	1.7
3	392	Typic Udipsamment	No	3–4	No	Loamy sand	1.3	2.5
4	517	Typic Udipsamment	No	4	No	Sand	0.9	1.3
6	787	Typic Udipsamment	No	15–20	No	Sand	0.9	2.7
8	1826	Spodic Udipsamment	Yes	5	No	Loamy sand	2.7	0.3
11	3384	Spodic Udipsamment	Yes	12	No	Loamy sand	4.0	0.3
12	3903	Typic Placorthod	Yes	8	Yes	Loamy sand	1.2	1.2
13	4422	Typic Placorthod	Yes	4	Yes	Loamy sand	2.1	1.2
15	5461	Typic Placorthod	Yes	4	Yes	Loamy sand	2.7	0.8
17	6500	Typic Placorthod	Yes	15	Yes	Loamy sand	0.7	0.5

nd, not determined.
[a] Determined in the B horizon of the profile pits on each dune by extraction in 0.1 M $BaCl_2$.
[b] Determined in the upper 20 cm of mineral soil in the profile pits on each dune by extraction in 0.1 M $BaCl_2$.

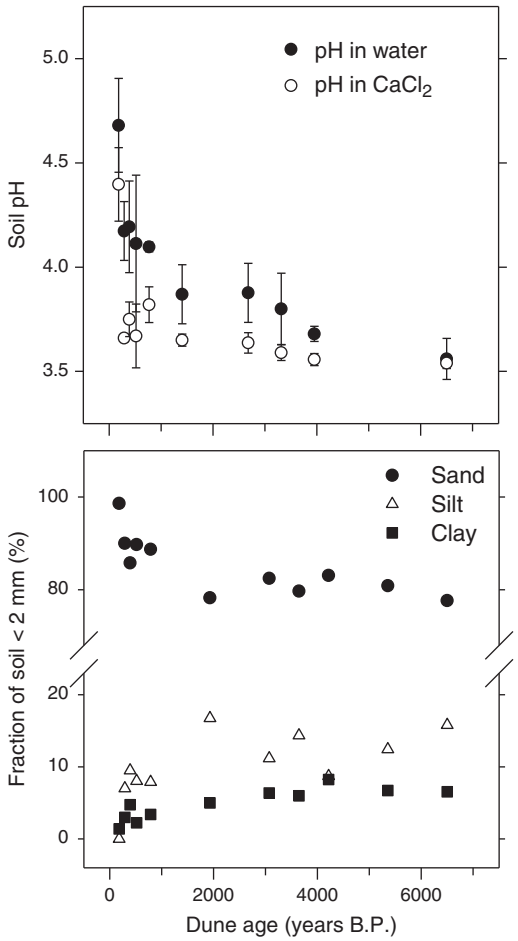

Fig. 3. Changes in pH and particle-size fractions (sand, silt, and clay) in the upper mineral soil (0–20 cm) along the Haast dune sequence, New Zealand. Values for soil pH are the mean ± standard error of three replicate plots located along the dune crest at each site, while values for texture are means of genetic horizons contributing to the upper 20 cm of mineral soil from a single profile pit on each dune.

of bases (<0.1 $cmol_c\ kg^{-1}$ for calcium, magnesium and sodium; ≤0.7 $cmol_c\ kg^{-1}$ for potassium). In C horizons the effective cation exchange capacity was extremely low on almost all dunes (<1 $cmol_c\ kg^{-1}$).

4.3. Profile weights of carbon, nitrogen, and phosphorus in mineral soil

The majority of the carbon and nitrogen was contained in the upper parts of the soil profile (Table 3, Fig. 4). Carbon in the upper meter of mineral soil increased throughout the sequence until Dune 13 (4422 years B.P.), where it reached 15 kg C m^{-2}, before declining to <10 kg C m^{-2} on the oldest dune (Table 3). Nitrogen followed a slightly different trend, reaching high values of 530 g m^{-2} on Dune 3 (392 years B.P.) and 613 g N m^{-2} on Dune 17 (~6500 years B.P.). The trends in carbon and nitrogen were reflected in an increase in the C:N ratio of the upper meter of mineral soil, which reached a maximum of 33.2 by Dune 13 and then declined to 15.7 on the oldest dune (Table 3).

In contrast to carbon and nitrogen, the majority of the phosphorus was contained in deep soil horizons, and the weight of total phosphorus in the upper meter of mineral soil did not show a clear trend through time (Fig. 4). Profile weights of phosphorus > 400 g P m^{-2} were recorded on both young and old dunes, while the lowest value (151 g P m^{-2}) occurred on Dune 12 (3903 years B.P.) (Table 3), which contained a deep and relatively phosphorus-poor B horizon.

Table 3
Profile weights of total elements in the mineral soil to 1 m depth at eleven sites along the Haast dune sequence, New Zealand.

Dune stage	Dune age (years B.P.)	Profile weight			Elemental ratio (by mass)	
		Carbon	Nitrogen	Phosphorus	C/N	C/P
		——————g m^{-2}——————				
1	181	2608	231	413	11.3	6.3
2	290	6926	452	253	15.3	27.4
3	392	8800	530	429	16.6	20.5
4	517	8262	400	291	20.7	28.4
6	787	8668	430	393	20.2	22.1
8	1826	8765	343	330	25.6	26.6
11	3384	10,962	364	272	30.1	40.3
12	3903	14,573	488	151	29.9	96.5
13	4422	15,039	453	415	33.2	36.2
15	5461	10,378	449	210	23.1	49.4
17	6500	9594	613	473	15.7	20.3

Values in parentheses are the proportion (%) of the total phosphorus.

4.4. Organic horizon thickness and element content

The organic horizon was relatively shallow on young dunes (<1 to 6 cm), but thickened markedly after Dune 6 (787 years B.P.) to between 17 and 28 cm (Table 4). As a result, the mass of carbon, nitrogen, and phosphorus in the organic horizon increased from low values on young dunes to maximum values by Dune 13 (4422 years B.P.) (Table 4). Values then declined on the oldest dune; this was driven mainly by a decline in the depth of the organic horizon, because element concentrations increased in the organic horizon on this dune (see below).

Carbon and nitrogen in the organic horizon constituted <10% of the total profile weight (i.e., organic plus mineral soil to 1 m depth; see below) of these elements on young dunes (<1000 years old), but >10% (and usually around 20%) of the total profile weight for older dunes (>1000 years old) (Table 4). In contrast, phosphorus in the organic horizon was always <2% of the total profile weight of phosphorus.

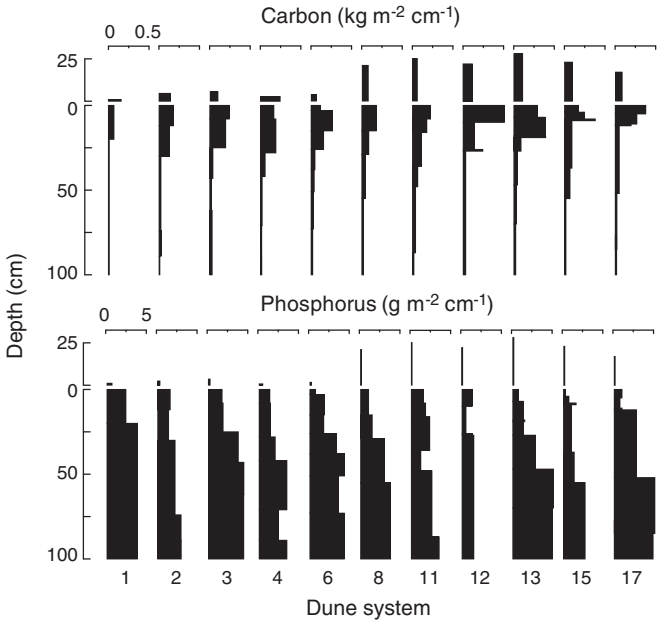

Fig. 4. The distribution of carbon and phosphorus to 1 m depth in eleven profiles along a sand dune chronosequence at Haast, New Zealand. The organic horizons are also shown. Nitrogen follows a similar pattern to carbon and is not shown. Dates of the dunes are shown in Table 1.

Table 4
Depth and total elemental contents of the organic horizon along the Haast dune sequence, New Zealand. Values for the depth are the mean ± standard error of five replicate measurements on each dune. Element mass calculated from mean concentrations determined in three replicate plots and bulk density from the profile pit at each dune stage.

Dune stage	Dune age (years B.P.)	Organic horizon depth[a] —cm—	Element mass		
			Carbon	Nitrogen	Phosphorus
			————————g m^{-2}————————		
1	181	<1	188	9.0	0.73
2	290	5 ± 0.4	771	19.8	1.42
3	392	6 ± 0.7	627	19.8	1.36
4	517	3 ± 0.5	808	22.3	1.47
6[b]	787	4 ± 0.5	282	9.1	0.72
8	1826	21 ± 1	1809	57.9	2.25
11	3384	25 ± 4	1662	53.0	2.08
12	3903	22 ± 1	2953	87.2	2.93
13	4422	28 ± 2	3610	107.7	3.85
17	6500	17 ± 3	1695	47.8	2.03

[a] Mean ± standard error of five replicate samples from the upper backslope of the dune.
[b] Incipient organic horizon on this dune, but this was included in the mineral soil (0–3 cm).

4.5. Total element concentrations in organic and surface mineral soils

Concentrations of carbon and nitrogen followed similar trends along the sequence in both organic and upper mineral soils (0–20 cm) (Fig. 5). In the organic horizon, carbon and nitrogen concentrations increased from low values in the young dunes to maximum and stable values in the older dunes, with a slight decline in the total nitrogen concentration with age. In surface mineral soil there was an initial rapid increase in carbon and nitrogen concentrations to maximum values by Dune 6 (787 years B.P.), then a decline to lower and stable values for the remainder of the sequence.

In contrast, total phosphorus concentrations in both organic and surface mineral soil horizons declined rapidly in the first few hundred years of pedogenesis from high initial values on young dunes to low values on old dunes (Fig. 5). In the organic horizon, the total phosphorus concentration declined approximately two-fold, from 885 ± 106 mg P kg^{-1} on the youngest dune to 485 ± 17 mg P kg^{-1} on Dune 12 (3903 years B.P). Total P then increased again on the oldest dune to 611 ± 15 mg P kg^{-1}. In surface mineral soil, the total phosphorus concentration declined three-fold, from 311 ± 17 mg P kg^{-1} on the youngest dune, to 102 ± 1 mg P kg^{-1} on Dune 17 (6500 years B.P.). The pattern of total phosphorus concentrations therefore differed markedly from that of the profile weights of phosphorus to 1 m depth.

4.6. Inorganic and organic phosphorus concentrations in the upper mineral soil

Much of the decline in total phosphorus in the early stages of pedogenesis was accounted for by acid-extractable inorganic phosphorus, which declined rapidly from 258 ± 49 mg P kg^{-1} on the youngest dune to <70 mg P kg^{-1} in the first few hundred years (Fig. 6). It then declined further, reaching ≤20 mg P kg^{-1} on the three oldest dunes. Initial parent material (beach sand) contained an acid-extractable inorganic phosphate concentration of 297 mg P kg^{-1}. Of the total phosphorus in the surface mineral soil, 80% was inorganic in the youngest dune, declining rapidly to ≤20% in the older dunes (Fig. 6).

At the same time, organic phosphorus increased from 54 ± 38 mg P kg^{-1} on the youngest dune to a maximum of 180 ± 5 mg P kg^{-1} on Dune 6 (787 years B.P.). It then declined slowly over the next several thousand years, reaching 82 ± 1 mg P kg^{-1} on the oldest dune. Organic phosphorus accounted for 72–84% of the total phosphorus for all but the youngest dune (Fig. 6). It was therefore the dominant form of phosphorus in the surface mineral soil for >6000 years.

4.7. Total element ratios in organic and surface mineral horizons

The C:N ratio in mineral soil increased steadily throughout the sequence from 13 ± 1 in the youngest soil to >20 in the oldest soils (Fig. 7). In the organic horizon the C:N ratio was always >30, apart from the youngest dune. The C:P ratio in mineral soil increased initially to a maximum of 154 ± 21 on Dune 2 (290 years B.P.), declined, and then increased to ≥200 in the three oldest dunes. Values in the organic horizon were much higher, increasing from 263 ± 45 on the youngest dune to 1008 ± 40 on Dune 12 (3903 years B.P.). The N:P ratio in mineral soil followed a similar trend to the C:P ratio, increasing initially to 8.6 ± 0.4 on Dune 2 (290 years B.P.), declining, and then increasing steadily to a maximum of ~10 in the two oldest dunes. Values in the organic horizon increased from 12–15 on young dunes (181–787 years B.P.) to 24–30 on older dunes (1826–6500 years B.P.) (Fig. 7). The ratios of carbon to organic phosphorus and nitrogen to organic phosphorus showed a different trend to C:P and N:P ratios. Values initially declined in the first 2000 years, before increasing steadily to maximum values on the oldest two dunes (Fig. 6).

4.8. Extractable inorganic nitrogen and phosphate

Phosphate extracted by anion-exchange membrane was highest in the young dunes (3.8–6.6 mg P kg^{-1}). It then declined steadily in the older dunes to the lowest value (0.7 mg P kg^{-1}) on Dune 17 (~6500 years B.P.) (Fig. 8).

For soils sampled in 2007 and extracted after several days of storage, concentrations of ammonium increased with dune age on the younger dunes to a maximum of 6.5 mg N kg^{-1} on Dune 6 (787 years B.P.), then remained at 2.0–3.7 mg N kg^{-1} in older dunes (Fig. 8). In contrast, nitrate was present in a significant amount only in the youngest dune (10 mg N kg^{-1}). For soils sampled in 2008 and extracted in the field, no nitrate or ammonium was detected in any sample (detection limit 1 mg N kg^{-1}).

5. Discussion

5.1. Soil development along the Haast chronosequence

Soils along the Haast chronosequence demonstrate a clear pedogenic trend of podzol development, from weakly-developed Entisols on young dunes, to well-developed Spodosols on old dunes. Podzol formation involves the mobilization and eluviation of aluminum and iron from upper soil horizons driven by the production of organic acids from decomposing plant material, and the immobilization of these metals in short-range-order complexes with organic matter in the B horizon (Buol et al., 2003). The Spodosols at Haast are typified by thick organic horizons, bleached eluvial (albic) horizons, illuvial (spodic) B horizons, and a continuous cemented iron pan (placic horizon). This occurred relatively rapidly under the perudic rainfall regime at Haast, with the albic horizon forming in <2000 years and the placic horizon forming in <4000 years. The development of a Bh horizon above the iron pan in the three oldest soils at Haast presumably indicates the impediment of vertical water movement by the iron pan, leading to the accumulation of organic matter in the lower part of the albic horizon after >4000 years of pedogenesis.

Podzol development has been studied extensively using soil chronosequences. For example, Stevens and Walker (1970) and Jenny (1941) summarize a series of early studies of sand dune chronosequences from Sweden, England, and elsewhere. An extreme example is the sand dune sequences along the east coast of Australia, including the well-studied Cooloola sequence, which develop into 'giant humus podzols', with bleached horizons >15 m deep over thick spodic

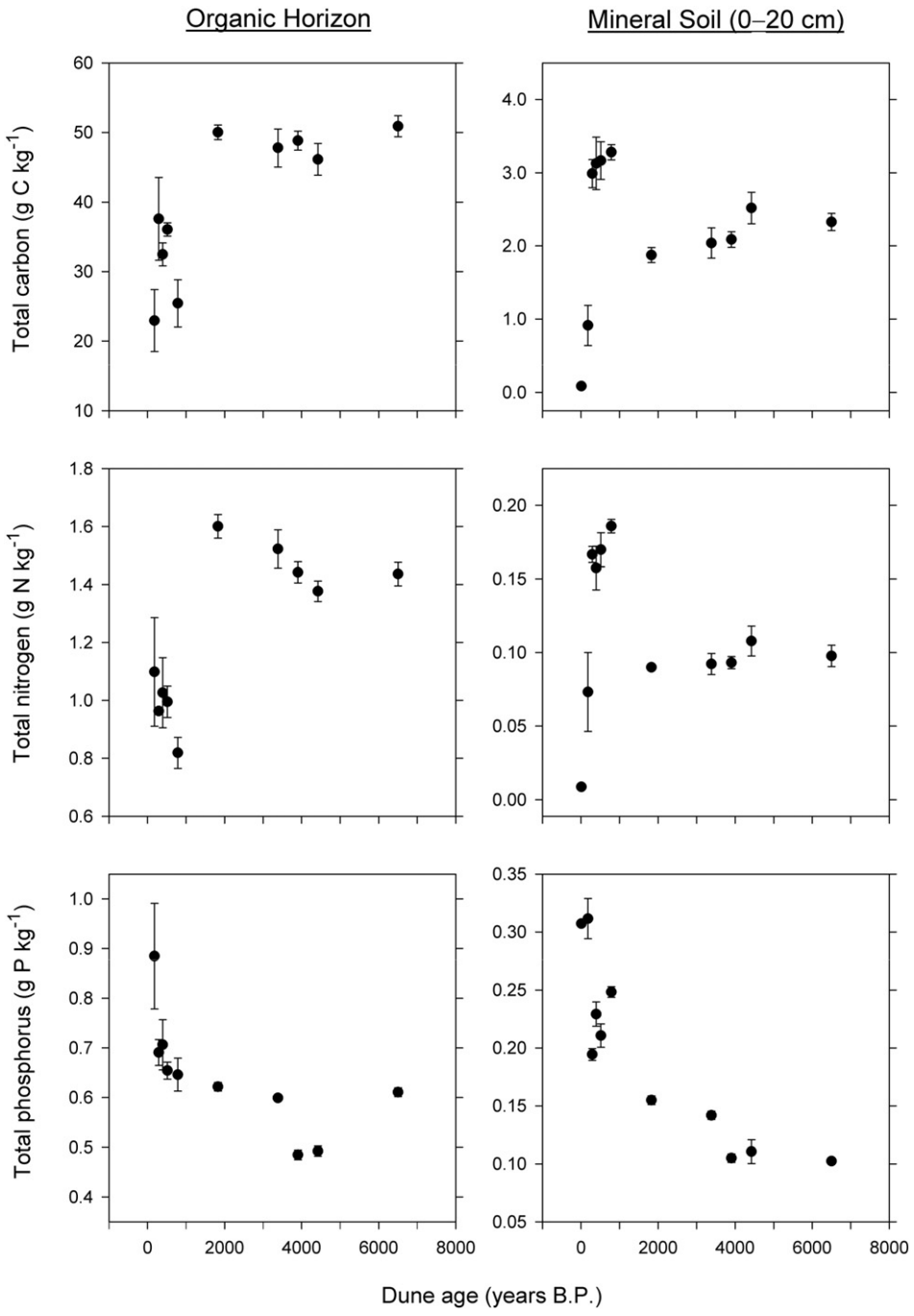

Fig. 5. Concentrations of carbon, nitrogen, and phosphorus in the organic horizon and the upper mineral soil (0–20 cm) along the Haast dune sequence, New Zealand. Values are the mean ± standard error of three replicate plots located along the dune crest at each site.

horizons (Thompson, 1981). A detailed study of podzol development was conducted on the Lake Michigan sand dune chronosequence (Lichter, 1998). In New Zealand, a similar pedogenic trend to that at Haast has been reported for soils developed on contrasting parent materials in the Westland region (e.g., Almond and Tonkin, 1999; Campbell, 1975; Ross et al., 1977; Smith and Lee, 1984; Stevens, 1968; Tonkin and Basher, 2001). All show a similar transition from Entisols to Spodosols, but the rate of development increases markedly with annual rainfall. For example, soils developed in coastal sand dunes of the Manawatu chronosequence with <1000 mm of annual rainfall show no signs of podzol formation in 10,000 years (Molloy, 1988). Tonkin and Basher (2001) note that under 2000 mm of annual rainfall albic horizons develop after 14,000–20,000 years of pedogenesis, whereas under 10,000 mm of annual rainfall the same process occurs in only 1000 years.

The development of a placic horizon is almost always associated with sandy soils developing under a udic or perudic moisture regime. For example, placic horizons do not occur along the Cooloola sequence under ~1500 mm rainfall (Thompson, 1981). At Haast, under ~3500 mm of annual rainfall, a placic horizon developed after >3384 years of pedogenesis, while in the Cropp River Basin in northern Westland, on gentle slopes of schist colluvium under 10,000 mm of rainfall, the development of Typic Placorthods (i.e., Spodosols with a cemented iron pan) occurred after only ca. 1500 years (Tonkin and Basher, 2001). It is likely that the formation of a placic horizon has ecological significance at Haast, because it impedes root growth and restricts water flow in the otherwise

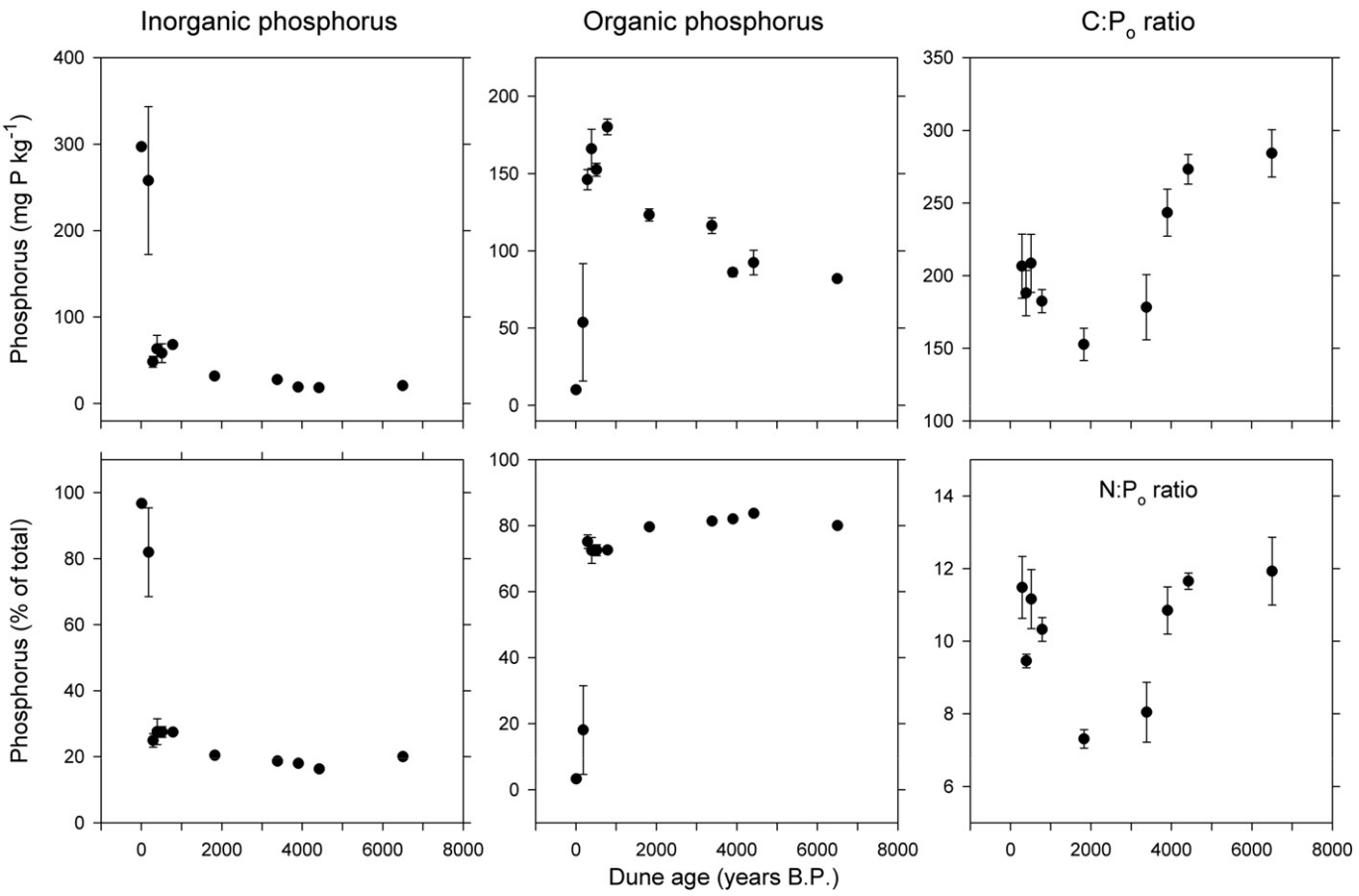

Fig. 6. Concentrations of inorganic and organic phosphorus, and the ratios of carbon and nitrogen to organic phosphorus, in the upper mineral soil (0–20 cm) along the Haast dune sequence, New Zealand. Values are the mean ± standard error of three replicate plots located along the dune crest at each site.

free-draining sandy soils (Palmer et al., 1986). Indeed, few roots were observed in deeper parts of the profiles, despite abundant phosphorus (see below).

In terms of nutrients, waterlogging might promote phosphorus availability in the short-term through reduction of iron oxides and solubilization of associated phosphate, but could exacerbate phosphorus depletion in the longer-term if the solubilized phosphorus is lost by leaching. Indeed, organic phosphorus, which is the dominant form of phosphorus on old soils, can be especially vulnerable to loss from the soil by leaching, because it can be more mobile in the soil profile than inorganic phosphate (Turner, 2005). Waterlogged conditions resulting from the formation of an iron pan on the marine uplift terraces at Waitutu appears to influence the patterns of vegetation communities by favoring flood-tolerant species (Gaxiola et al., 2010). Pan formation is also significant on the old marine terraces of the Mendocino chronosequence in California, where podzolized soils several hundred thousand years old with iron pans and impeded drainage support stunted conifer forest (Jenny et al., 1969).

5.2. Dune disturbance and soil development at Haast

The integrity of a chronosequence depends on soils at each site having undergone minimal disturbance. Significant disturbance at Haast could include tree falls, which can have a considerable influence on the development of podzols (Norton, 1989), or some degree of reworking such as erosion or deposition of material onto dune ridges. A buried albic horizon in Dune 11 indicates that at least some of the dunes may have undergone some form of disturbance, although the spatial extent of this is unknown given that only a single profile pit was studied on each dune. There is an increased likelihood of loess deposition as dunes age; this is common in the Westland region and brings weakly-weathered material into the system, which is expected to enhance phosphorus availability and nutrient availability and complicate interpretation of pedogenic processes and rates (Almond et al., 2001). The likelihood of disturbance and loess deposition on older dunes is supported by climatic changes that occurred around 3000 years B.P. Based on pollen records from a nearby marsh, Li et al. (2008) inferred a significant drying in the Haast region around 3700 years B.P. (see Methods). This is similar to the estimated age of Dune 11 (3384 years B.P.) and may therefore explain the unusual features of the soil profile on that dune.

5.3. Changes in soil nutrients during pedogenesis: profile weights of total elements

Changes in the profile weights of total carbon and total nitrogen in mineral soil generally followed the expected trend based on previous chronosequence studies in the region and elsewhere, with a marked accumulation of organic matter in the upper soil horizons in the early stages of pedogenesis, followed by a slight decline in the older stages (Peltzer et al., 2010; Syers and Walker, 1969; Walker and Syers, 1976). The amounts of carbon and nitrogen in the organic horizon followed a similar trend, accumulating through time as the thickness of the organic horizon increased, although there was a decline on the oldest dune, consistent with more rapid decomposition due to an increase in nutrient availability (see above).

The profile weights of total phosphorus did not, however, follow the expected decline through time. This appears to be in large part

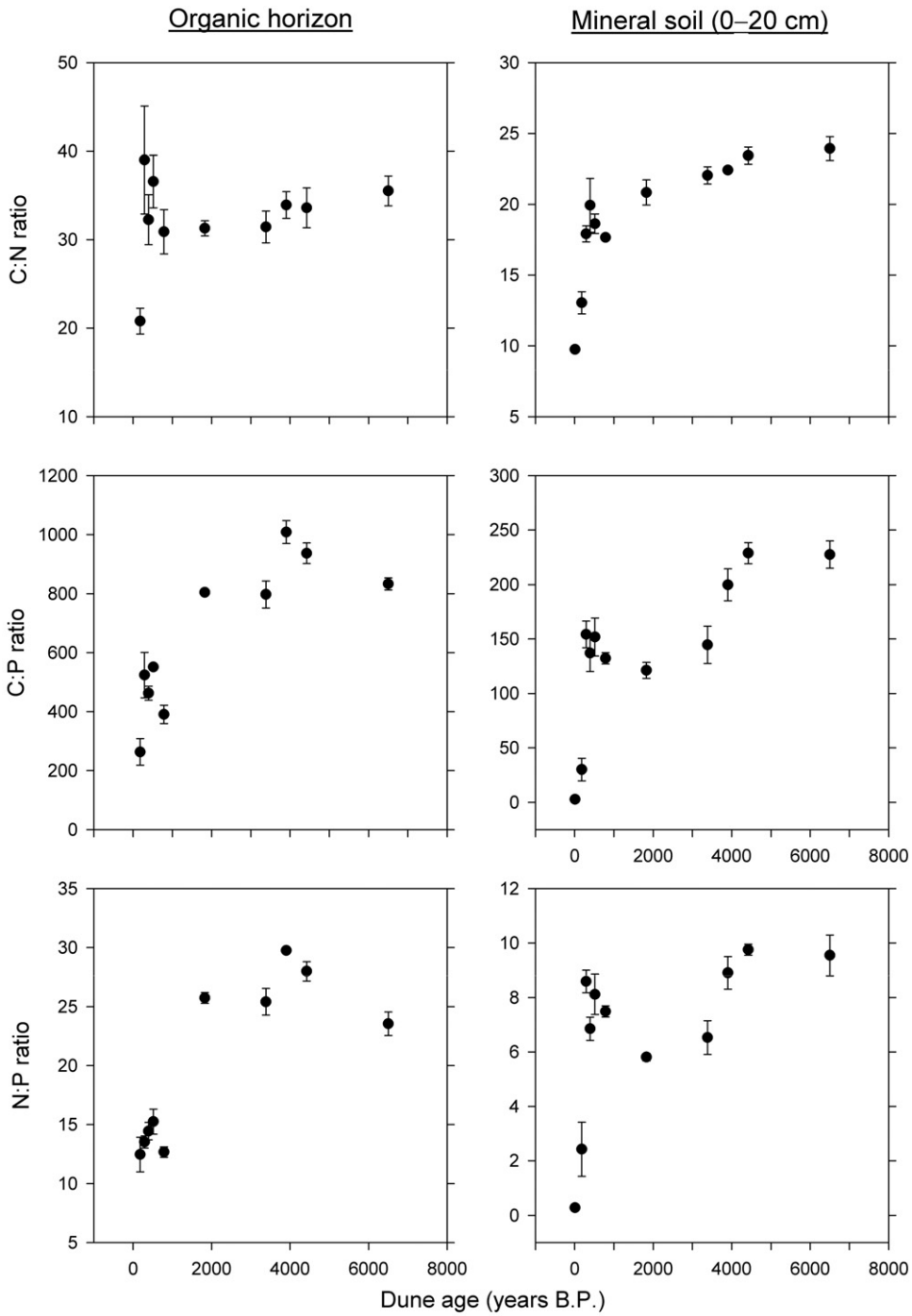

Fig. 7. Total element ratios for carbon, nitrogen, and phosphorus in the organic horizon and the upper mineral soil (0–20 cm) along the Haast dune sequence, New Zealand. Values are the mean ± standard error of three replicate plots located along the dune crest at each site.

due to the variable amounts of phosphorus in the deeper parts of the profiles where the majority of the phosphorus occurs and presumably indicates differences among the dunes in properties such as parent material, proximity to the water table, and the extent of disturbance. As a result, the profile-weighted C:P and N:P ratios did not show clear increases through time, as expected from the Walker and Syers (1976) model of stoichiometric transformations during pedogenesis. In this respect the Haast sequence differs from the Manawatu sand dune chronosequence on the North Island of New Zealand. Although changes in total phosphorus contents were variable along the sequence, there was an estimated loss of 1910 kg P ha^{-1} of total phosphorus from the top meter of the profile over 10,000 years, with a parallel accumulation of 1050 kg P ha^{-1} in organic forms (Syers and Walker, 1969). In contrast, an erratic pattern of total phosphorus occurred in profiles along both the Franz Josef sequence (Walker and Syers, 1976) and the Hawaiian Island sequence (Crews et al., 1995), where in both cases phosphorus contents in the fine earth fraction peaked in intermediate-aged soils. Soil phosphorus showed little change along a chronosequence of coastal sand dunes in Georgia, USA (Tackett and Craft, 2010), where nitrogen availability appeared to be the strongest constraint on biological activity, as expected from the relatively young age of the sequence.

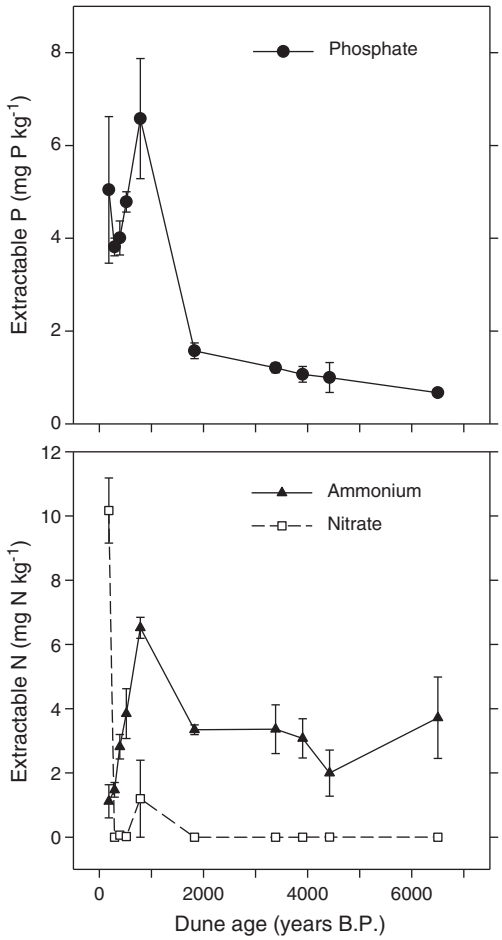

Fig. 8. Changes in extractable (plant-available) nitrogen and phosphate in the upper mineral soil (0–20 cm) along the Haast dune sequence, New Zealand. Values are the mean ± standard error of three replicate plots located along the dune crest at each site.

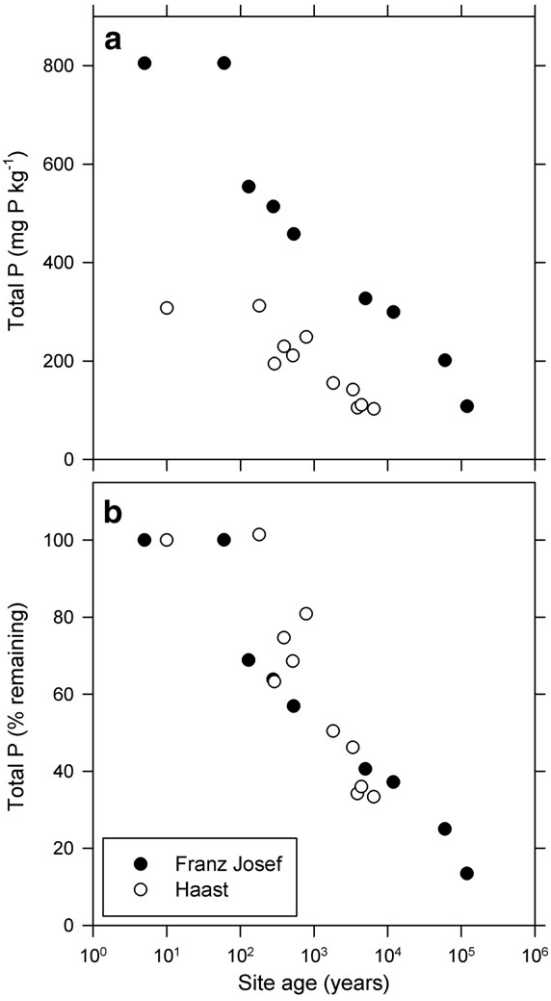

Fig. 9. Comparison of changes in total phosphorus with soil age along the Haast dune sequence and the Franz Josef post-glacial sequence, showing (A) the decline in total phosphorus and (B) the proportion (%) of the total phosphorus remaining. Data for the Franz Josef sequence are from Richardson et al. (2004). Values for percent remaining are based on total phosphorus concentrations in the youngest sample (beach sand for Haast and 5-year surface for Franz Josef).

5.4. Changes in soil nutrients during pedogenesis: total element concentrations

Although the Walker and Syers (1976) model is based on changes in total phosphorus on a profile basis, many of the reports of changes in phosphorus through time have focused on concentrations in the surface soil rather than weights of phosphorus in the whole profile (e.g., Parfitt et al., 2005; Richardson et al., 2004; Wardle et al., 2004). At Haast, total phosphorus concentrations in surface mineral soil and the organic horizon followed a clear trend of depletion through time, as reported in a number of previous studies on chronosequences in New Zealand and elsewhere (reviewed in Peltzer et al., 2010). In this sense, the Haast sequence follows the expected trend of phosphorus availability during ecosystem development (i.e., a progressive depletion of phosphorus in the rooting zone of plants), with consequences for forest biomass and productivity (Wardle et al., 2004).

In a study of phosphorus in three long-term chronosequences developed on contrasting parent materials in New Zealand, Parfitt et al. (2005) reported total phosphorus concentrations in mineral soils declined at a relatively similar rate in different soils, including the Franz Josef post-glacial sequence, the Waitutu marine uplift terraces, and a volcanic sequence. In Fig. 9 we compare rates of phosphorus decline at Haast and Franz Josef. We did not include data on the other two sequences reported in Parfitt et al. (2005), because they do not include young soils where phosphorus depletion occurs most rapidly. For the Franz Josef post-glacial chronosequence developed in coarse graywacke under 3600–6600 mm annual rainfall, total phosphorus concentrations were ~800 mg P kg^{-1} on the youngest surfaces, declining to ~100 mg P kg^{-1} after 120,000 years (Fig. 9A; Parfitt et al., 2005; Richardson et al., 2004). In contrast, total phosphorus concentrations in the early stages of the Haast chronosequence developed in schist-derived sand under ~3500 mm annual rainfall were ~300 mg P kg^{-1} and declined to ~100 mg P kg^{-1} after only around 4000 years (Fig. 9A). When phosphorus loss was expressed as the percent decline from initial values, however, the rates of decline at Haast and Franz Josef were remarkably similar, with 50% of the phosphorus lost after ~1000 years in both sequences (Fig. 9B). We conclude that the rapid decline in total phosphorus concentrations in mineral soil along the Haast chronosequence compared to nearby sites is driven in large part by differences in parent material (e.g., initial phosphorus concentrations, particle-size class, etc.), although proportional losses of phosphorus can occur at a similar rate in very different systems. The latter observation warrants further attention, because it offers the possibility of reconciling patterns of phosphorus depletion across systems with markedly different soils and phosphorus contents.

Organic and inorganic phosphorus concentrations in the upper mineral soil also changed predictably along the Haast chronosequence, consistent with the Walker and Syers (1976) model. In particular, there was an initial rapid decline in primary mineral phosphate following the onset of pedogenesis, and a simultaneous accumulation in organic

phosphorus, the latter becoming the dominant component of the total phosphorus within a few hundred years. These changes in the Haast chronosequence are similar to other sequences in the region (Parfitt et al., 2005; Wardle et al., 2004), including those on river terraces (Ross et al., 1977; Smith and Lee, 1984), moraines (Richardson et al., 2004; Turner et al., 2007; Walker and Syers, 1976), and marine uplift terraces (Coomes et al., 2005). The significance of organic phosphorus as a source of biologically-available phosphorus is highlighted here, even on moderately weathered soils, because the majority of the total phosphorus is in this form in Haast soils after only a few hundred years of pedogenesis. Although a small proportion of this pool is likely to be inorganic phosphate occluded within secondary minerals (Turner et al., 2007; Williams and Walker, 1967), it seems certain that trees depend on the turnover of soil organic phosphorus for their phosphorus nutrition along the majority of the Haast chronosequence.

When considered in the organic horizon and upper mineral soil, the C:P and N:P ratios generally increased through time, indicative of increasing phosphorus limitation during pedogenesis. The rate of change in the C:organic P ratio in mineral soils along the Haast sequence, reaching a ratio of ~300 after about 4000 years, was consistent with the three sequences studied by Parfitt et al. (2005). There were also parallel changes in available phosphate, with a rapid decline to low concentrations in the early stages of pedogenesis. Less can be said about nitrogen availability given the undetectable concentrations in freshly-extracted soils at all stages of the sequence. The inorganic nitrogen measurements made after storage may, however, reflect differences in nitrogen mineralization rates, in which case nitrogen availability appears to be greater in younger dunes. Despite the apparent increasing degree of phosphorus limitation on older soils, there appeared to be considerable amounts of phosphorus available in subsoils on old dunes. However, the iron pan appears to restrict root access to these deeper horizons.

6. Conclusions

Rapid podzol development in sandy soils along the Haast chronosequence in New Zealand involves a marked decline in phosphorus concentrations in surface soils, acidification and depletion of base cations, accumulation of organic matter including a thick organic horizon, and formation of a continuous, cemented iron pan. The initial decline in total phosphorus is associated with the disappearance of primary mineral phosphate, and organic phosphorus accounts for the majority of the phosphorus in the upper mineral soil for the majority of the 6500 years of the sequence. The Haast chronosequence differs from other nearby and well-studied sequences in terms of parent material, soil texture, and initial phosphorus concentration, and therefore provides an important additional example of pedogenesis linked to long-term soil phosphorus depletion.

Acknowledgments

We thank Peter Almond, Amanda Black, Victoria Nall, and Andre Eger (Lincoln University) for field assistance, Ellis Benham (USDA–NRCS, Lincoln, NE) for advice on soil classification, and Tania Romero, Luis Ramos, Dianne de la Cruz, and Dayana Agudo (STRI) for laboratory assistance. Kelly Andersen was supported by a Smithsonian Institution Postdoctoral Fellowship. Funding for travel and consumables was provided by Lincoln University.

Appendix A. Supplementary data

Two files containing profile descriptions and data on chemical and physical properties by genetic horizons are provided online as supplementary files. The files are also available along with profile photos at: http://www.stri.si.edu/sites/soil/soildatabase/. Supplementary data to this article can be found online at http://dx.doi.org/10.1016/j.catena.2012.05.007.

References

Almond, P.C., Tonkin, P.J., 1999. Pedogenesis by upbuilding in an extreme leaching and weathering environment, and slow loess accretion, south Westland, New Zealand. Geoderma 92, 1–36.
Almond, P.C., Moar, N.T., Lian, O.B., 2001. Reinterpretation of the glacial chronology of South Westland, New Zealand. New Zealand Journal of Geology and Geophysics 44, 1–15.
Buol, S.W., Southard, R.J., Graham, R.C., McDaniel, P.A., 2003. Spodosols: soils with subsoil accumulations of humus and sesquioxides, Soil Genesis and Classification, fifth edition. Blackwell Publishing, Ames, Iowa, pp. 327–338.
Campbell, A.S., 1975. Chemical and Mineralogical Properties of a Sequence of Terrace Soils near Reefton, New Zealand. PhD thesis, University of Canterbury, New Zealand.
Cheesman, A.W., Turner, B.L., Reddy, K.R., 2010. Interaction of phosphorus compounds with anion-exchange membranes: implications for soil analysis. Soil Science Society of America Journal 74, 1607–1612.
Coomes, D.A., Bellingham, P.J., 2011. Temperate and tropical podocarps: how ecologically alike are they? In: Turner, B.L., Cernusak, L.A. (Eds.), Ecology of the Podocarpaceae in Tropical Forests. Contributions to Botany No. 95. Smithsonian Institution Scholarly Press, Washington, D.C, pp. 119–140.
Coomes, D.A., Allen, R.B., Bentley, W.A., Burrows, L.E., Canham, C.D., Fagan, L., Forsyth, D.M., Gaxiola-Alcantar, A., Parfitt, R.L., Ruscoe, W.A., Wardle, D.A., Wilson, D.J., Wright, E.F., 2005. The hare, the tortoise and the crocodile: the ecology of angiosperm dominance, conifer persistence and fern filtering. Journal of Ecology 93, 918–935.
Crews, T.E., Kitayama, K., Fownes, J.H., Riley, R.H., Herbert, D.A., Mueller-Dombois, D., Vitousek, P.M., 1995. Changes in soil phosphorus fractions and ecosystem dynamics across a long chronosequence in Hawaii. Ecology 76, 1407–1424.
Gaxiola, A., McNeill, S.M., Coomes, D.A., 2010. What drives retrogressive succession? Plant strategies to tolerate infertile and poorly drained soils. Functional Ecology 24, 714–722.
Gee, G.W., Or, D., 2002. Particle size analysis. In: Dane, J.H., Topp, C. (Eds.), Methods of Soil Analysis, Part 4 — Physical Methods. Soil Science Society of America, Madison, WI, pp. 255–293.
Gellatly, A.F., Chinn, T.J.H., Röthlisberger, F., 1988. Holocene glacier variations in New Zealand—a review. Quaternary Science Reviews 7, 227–242.
Griffiths, G.A., 1979. High sediment yields from major rivers of the western Southern Alps, New Zealand. Nature 282, 61–63.
Hedin, L.O., Vitousek, P.M., Matson, P.A., 2003. Nutrient losses over four million years of tropical forest development. Ecology 84, 2231–2255.
Hendershot, W.H., Lalande, H., Duquette, M., 2008. Chapter 18. Ion exchange and exchangeable cations. In: Carter, M.R., Gregorich, E. (Eds.), Soil Sampling and Methods of Analysis. Canadian Society of Soil Science and CRC Press, Boca Raton, FL, pp. 173–178.
Jenny, H., 1941. Factors of Soil Formation: A System of Quantitative Pedology. McGraw-Hill, New York.
Jenny, H., Arkley, R.J., Schultz, A.M., 1969. The pygmy forest-podzol ecosystem and its dune associates of the Mendocino coast. Madrono 20, 60–74.
Li, X., Rapson, G.L., Flenley, J.R., 2008. Holocene vegetational and climatic history, Sponge Swamp, Haast, south-western New Zealand. Quaternary International 184, 129–138.
Lichter, J., 1998. Rates of weathering and chemical depletion in soils across a chronosequence of Lake. Michigan sand dunes. Geoderma 85, 255–282.
Loeppert, R.H., Inskeep, W.P., 1996. Iron. In: Sparks, D.L., et al. (Ed.), Methods of Soil Analysis, Part 3 — Chemical Methods. Soil Science Society of America, Madison, WI, pp. 639–664.
McGlone, M.S., Wilmshurst, J.M., 1999. A Holocene record of climate, vegetation change and peat bog development, east Otago, South Island, New Zealand. Journal of Quaternary Science 14, 239–254.
Menge, D.N.L., Hedin, L.O., 2009. Nitrogen fixation in different biogeochemical niches along as 120 000-year chronosequence in New Zealand. Ecology 90, 2190–2201.
Molloy, L., 1988. Soils of the New Zealand Landscape. New Zealand Society of Soil Science, Canterbury, New Zealand.
New Zealand Meteorological Service, 1983. Summaries of climatological observations to 1980. New Zealand Meteorological Service Miscellaneous Publication, 177. Canterbury, New Zealand, p. 172.
Norton, D.A., 1989. Tree windthrow and forest soil turnover. Canadian Journal of Forest Research 19, 386–389.
Palmer, R.W.P., Doyle, R.B., Grealish, G.J., Almond, P.C., 1986. Soil studies in south Westland, 1984/1985. Soil Bureau District Office Report NP 2. Department of Scientific and Industrial Research, New Zealand.
Parfitt, R.L., Ross, D.J., Coomes, D.A., Richardson, S.J., Smale, M.C., Dahlgren, R.A., 2005. N and P in New Zealand soil chronosequences and relationships with foliar N and P. Biogeochemistry 75, 305–328.
Peltzer, D.A., Wardle, D.A., Allison, V.J., Baisden, W.T., Bardgett, R.D., Chadwick, O.A., Condron, L.M., Parfitt, R.L., Porder, S., Richardson, S.J., Turner, B.L., Vitousek, P.M., Walker, J., Walker, L.R., 2010. Understanding ecosystem retrogression. Ecological Monographs 80, 509–529.
Porter, S.C., 2000. Onset of neoglaciation in the Southern Hemisphere. Journal of Quaternary Science 15, 395–408.
Richardson, S.J., Peltzer, D.A., Allen, R.B., McGlone, M.S., Parfitt, R.L., 2004. Rapid development of phosphorus limitation in temperate rainforest along the Franz Josef soil chronosequence. Oecologia 139, 267–276.

Ross, C.W., Mew, G., Searle, P.L., 1977. Soil sequences on two terrace systems in the north Westland area, New Zealand. New Zealand Journal of Science 20, 231–244.
Smith, S.M., Lee, W.G., 1984. Vegetation and soil development on a Holocene river terrace sequence, Arawata Valley, south Westland. New Zealand Journal of Science 27, 187–196.
Soil Survey Staff, 1999. Soil Taxonomy: A Basic System of Soil Classification for Making and Interpreting Soil Surveys. United States Department of Agriculture—Natural Resources Conservation Service, Lincoln, NE.
Stevens, P.R., 1968. A Chronosequence of Soils near The Franz Josef Glacier. PhD thesis, University of Canterbury, New Zealand.
Stevens, P.R., Walker, T.W., 1970. The chronosequence concept and soil formation. The Quarterly Review of Biology 45, 333–350.
Syers, J.K., Walker, T.W., 1969. Phosphorus transformations in a chronosequence of soils developed on wind-blown sand in New Zealand I. Total and organic phosphorus. Journal of Soil Science 20, 57–64.
Tackett, N.W., Craft, C.B., 2010. Ecosystem development on a coastal barrier island dune chronosequence. Journal of Coastal Research 736–742.
Thompson, C.H., 1981. Podzol chronosequence on coastal dunes of eastern Australia. Nature 291, 59–61.
Tonkin, P.J., Basher, L.R., 1990. Soil-stratigraphic techniques in the study of soil and landform evolution across the Southern Alps, New Zealand. Geomorphology 3, 547–578.
Tonkin, P.J., Basher, L.R., 2001. Soil chronosequences in subalpine superhumid Cropp Basin, western Southern Alps, New Zealand. New Zealand Journal of Geology and Geophysics 44, 37–45.
Turner, B.L., 2005. Organic phosphorus transfer from terrestrial to aquatic environments. In: Turner, B.L., Frossard, E., Baldwin, D.S. (Eds.), Organic Phosphorus in the Environment. CAB International, Wallingford, UK, pp. 269–294.
Turner, B.L., Romero, T.E., 2009. Short-term changes in extractable inorganic nutrients during transport and storage of tropical rain forest soils. Soil Science Society of America Journal 73, 1972–1979.
Turner, B.L., Condron, L.M., Richardson, S.J., Peltzer, D.A., Allison, V.J., 2007. Soil organic phosphorus transformations during pedogenesis. Ecosystems 10, 1166–1181.
Walker, T.W., Syers, J.K., 1976. The fate of phosphorus during pedogenesis. Geoderma 15, 1–19.
Walker, L.R., Wardle, D.A., Bardgett, R.D., Clarkson, B.D., 2010. The use of chronosequences in studies of ecological succession and soil development. Journal of Ecology 98, 725–736.
Wardle, D.A., Walker, L.R., Bardgett, R.D., 2004. Ecosystem properties and forest decline in contrasting long-term chronosequences. Science 305, 509–513.
Wells, A., Goff, J., 2006. Coastal dune ridge systems as chronological markers of palaeoseismic activity: a 650-yr record from southwest New Zealand. The Holocene 16, 543–550.
Wells, A., Goff, J., 2007. Coastal dunes in Westland, New Zealand, provide a record of paleoseismic activity on the Alpine fault. Geology 35, 731–734.
Wells, A., Duncan, R.P., Stewart, G.H., 2001. Forest dynamics in Westland, New Zealand: the importance of large, infrequent earthquake-induced disturbance. Journal of Ecology 89, 1006–1018.
Williams, J.D.H., Walker, T.W., 1967. Comparison of “ignition” and “extraction” methods for the determination of organic phosphate in rocks and soils. Plant and Soil 27, 457–459.
Williams, P.W., King, D.N.T., Zhao, J.X., Collerson, K.D., 2004. Speleothem master chronologies: combined Holocene ^{18}O and ^{13}C records from the North Island of New Zealand and their palaeoenvironmental interpretation. The Holocene 14, 194–208.